Chemistry & Biology
Article

A One-Pot Chemoenzymatic Synthesis for the Universal Precursor of Antidiabetes and Antiviral Bis-Indolylquinones

Patrick Schneider,[1] Monika Weber,[1] Karen Rosenberger,[1] and Dirk Hoffmeister[1,2,*]
[1] Pharmaceutical Biology and Biotechnology, Albert-Ludwigs-Universität, Stefan-Meier-Strasse 19, 79104 Freiburg, Germany
[2] Present address: University of Minnesota, Plant Pathology, 1991 Upper Buford Circle, St. Paul, MN 55108, USA.
*Correspondence: dirkh@umn.edu
DOI 10.1016/j.chembiol.2007.05.005

SUMMARY

Bis-indolylquinones represent a class of fungal natural products that display antiretroviral, antidiabetes, or cytotoxic bioactivities. Recent advances in *Aspergillus* genomic mining efforts have led to the discovery of the *tdiA-E*-gene cluster, which is the first genetic locus dedicated to bis-indolylquinone biosynthesis. We have now genetically and biochemically characterized the enzymes TdiA (bis-indolylquinone synthetase) and TdiD (L-tryptophan:phenylpyruvate aminotransferase), which, together, confer biosynthetic abilities for didemethylasterriquinone D to *Aspergillus nidulans*. This compound is the universal intermediate for all bis-indolylquinones. In this biochemical study of a bis-indolylquinone synthetase and a fungal natural product transaminase, we present a one-pot chemoenzymatic protocol to generate didemethylasterriquinone D in vitro. As TdiA resembles a nonribosomal peptide synthetase, yet catalyzes carbon-carbon-bond formation, we discuss the implications for peptide synthetase chemistry.

INTRODUCTION

Filamentous fungi represent a proven source for small-molecule drug lead structures that interact with various cellular targets [1]. Among fungal secondary metabolites, the bis-indolylquinone family of compounds has received close attention for three distinct bioactivities. First, cytotoxic effects in the submicromolar range, found in murine leukemia cell assays. This was shown for asterriquinone and derivatives [2]. Secondly, antiretroviral activity, e.g., anti-HIV activity, was found for didemethylasterriquinone D (DDAQ D), isocochliodinol, semicochliodinols A and B, and hinnuliquinone [3, 4] (Figure 1). These fungal natural products inhibit HIV-1-protease at concentrations of about 100–500 nM. The third bioactivity pertains to the antidiabetes activity of L 783,281 (didemethylasterriquinone B1) [5, 6] as this compound acts agonistically on the insulin receptor. Given the oral availability of this compound, this finding prompted increased interest in the bis-indolylquinones; protocols for their chemical synthesis were devised [7, 8]. The accepted hypothesis on bis-indolylquinone biosynthesis put forth by Arai and Yamamoto [9] includes deamination of L-tryptophan to indole-3-pyruvic acid, which feeds into a dimerization reaction to yield DDAQ D. This symmetric compound represents the generic intermediate en route to numerous derivatives, including the aforementioned compounds, whose pathways diverge due to regiospecific transfers of prenyl groups, the most prominent structural decorations of bis-indolylquinones. The C- or N-prenyltransfer reactions may occur symmetrically or disturb molecular symmetry by transfer of one single prenyl unit or two units to different acceptor positions.

More recently, the first genetic locus for a bis-indolylquinone metabolic pathway, the *tdiA-E* gene cluster (Figure 2) for terrequinone A, was discovered in the genome of the filamentous fungus *Aspergillus* (*A.*) *nidulans* applying genomic and chemical analyses along with microarray techniques [10]. Intriguingly, the translational products of two genes, *tdiD* and *tdiA*, resemble transaminases and an adenylation-thiolation-thioesterase/cyclase domain triad, respectively, the latter reminiscent to nonribosomal peptide synthetase (NRPS) domains. Based on these in silico analyses, we hypothesized that TdiD and TdiA could provide the key catalytic activities to expand the shikimic acid pathway beyond L-tryptophan toward DDAQ D.

In this publication, we report the genetic and biochemical characterization of the *tdiD*- and *tdiA*-encoded enzymes from *A. nidulans*, which represent the prototypical transaminase and bis-indolylquinone synthetase, respectively, for this class of natural products. To our knowledge, this is the first characterization of a bis-indolylquinone synthetase and a fungal natural product transaminase. Based on these results, we demonstrate a coupled TdiD/TdiA enzymatic one-pot reaction as a platform technology to provide the universal precursor for numerous bioactive bis-indolylquinones.

RESULTS

Sequencing of *tdiA* and *tdiD* cDNAs

The experimentally verified DNA-sequences for *tdiA* and *tdiD* deviate substantially from the predicted sequences

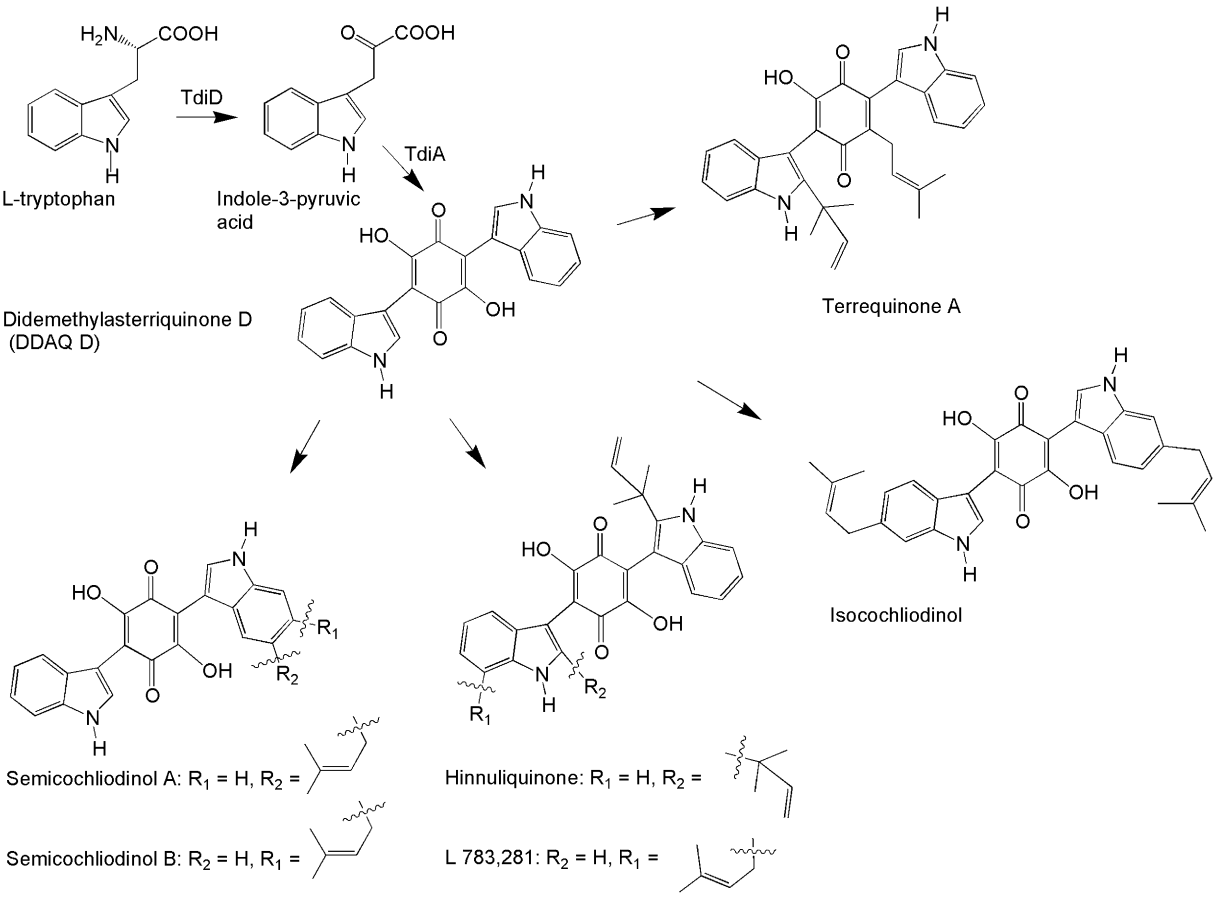

Figure 1. Chemical Structures of Bioactive Fungal Bis-Indolylquinones
Biosynthetic steps catalyzed by TdiA and TdiD are also shown.

deposited on the BROAD server [11], which relies on automatic computer-based gene annotation. For *tdiA*, a 63 bp intron is erroneously predicted in the 3′-terminal portion of the reading frame. Our results prove that *tdiA* is one continuous, intronless 2913 bp reading frame that codes for a 970 aa protein with a calculated mass of 107.6 kDa, which clearly presents sequence motifs for adenylation, peptidyl carrier, and thioesterase domains of NRPSs, as described by Marahiel and coworkers [12]: in TdiA, the thioesterase core motif ^{772}GYSFG^{776} follows exactly the consensus GxSxG, the peptidyl carrier protein (PCP) motif slightly deviates from the canonical sequence LGG(D/H)SL and is represented by ^{627}IGATSM^{632}. Of particular interest in our context was the adenylation domain, whose key residue amino acid 235 (according to PheA numbering) in core motif A4 [12] indicative for either amino (D235) or arylic (N235) acid activation replaced by a valine (V239) in TdiA (Table 1). Also, position 239 (in PheA numbering) was used in the past to discriminate dihydroxybenzoate (S239) from salicylate (C239) activating A-domains. This position, in turn, aligns with H244 in TdiA. It should be noted, however, that a cystein is residing at position 245.

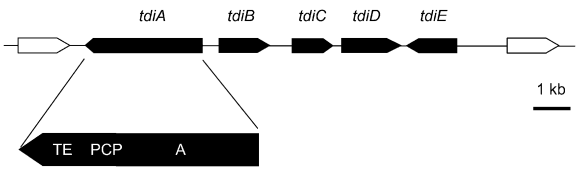

Figure 2. Organization of the Terrequinone A Biosynthetic Locus in *Aspergillus nidulans*
Black arrows indicate the transcriptional direction and symbolize the genetic cluster. Open arrows represent genes outside the cluster. The modular architecture of the *tdiA* gene product is highlighted by abbreviations: A (adenylation domain), PCP (peptidyl carrier protein), TE (thioesterase/cyclase).

We also report an updated *tdiD* sequence. By erroneously joining two adjacent contigs, 1.154 and 1.155, head to tail (rather than overlapping these), the gene *tdiD* was duplicated and, consequently, presented twice in the genome database as reading frames AN8516.3 and AN8519.3, both times annotated as "hypothetical gene." Confusingly, these sequences are not identical. Our *tdiD* cDNA sequence confirms AN8519.3 as correct

Table 1. Clustal W Alignment of the Adenylation Domain Portion around Core Motif A4 for TdiA, Its Homologs Found in Microbial Genomes, and Aryl Acid Adenylation Domains

Position		Enzyme
230	FL SWVHMDH**V**ANL V**H**C HI F AI	TdiA (*A. nid.*)
TdiA homologs		
218	TL NWI SF DH**V**AAL L**E**A HLL PL	*R. sol.*
217	FY NWVGL DH**V**ASL T**E**I HLHAL	*A. nid.*
233	FL SWVHMDH**V**ANL V**H**C HLF AI	*A. ter.*
221	FMSWVNMDH**V**ANL V**H**C HLF AI	*C. glob.*(1)
248	FL NWI GL DH**V**ASL V**E**MHI QAL	*C. glob.*(2)
236	FL SWVSF DH**S**AAL C**E**N HLHAV	*P. nod.*
Aryl acid adenylation		
213	YL CA LPV AH**N**FPL A**C**P GI L GT	YbtE
230	FL CA LPT AH**N**YPMS**S**P GAL GV	EntE
228	YL AA LPI AH**N**YPL S**S**P GVL GT	DhbE

The positions N235 and C239 (according to PheA numbering) are highlighted in bold. *R. sol.*: NP_522978 from *Ralstonia solanacearum*. In the shown region, the enzyme is identical to *Burkholderia pseudomallei* (accession number: YP_110151). *A. nid.*: AN3392.3 from *Aspergillus nidulans*. *A. ter.*: XP_001210786 from *Aspergillus terreus* NIH2624. *C. glob.* (1): XP_001230203 from *Chaetomium globosum* CBS 148.51. *C. glob.* (2): XP_001228818 from the same fungus. *P. nod.*: EAT88825 from *Phaeosphaeria nodorum* SN15. YbtE adenylates salicylic acid during yersiniabactin biosynthesis in *Yersinia pestis*, and EntE and DhbE adenylate 2,3-dihydroxybenzoic acid in the enterobactin pathway of *Escherichia coli* and the bacillibactin pathway of *Bacillus subtilis*, respectively.

version and also the existence of the 12 bp exon after base 435, which was lacking in the previous version AN8519.2 (and still is in AN8516.3). Therefore, *tdiD* represents a 1311 bp reading frame coding for a predicted 436 aa, 47.7 kDa member of the PLP-dependent aminotransferase family.

Gene Inactivations

The terrequinone A biosynthetic genes were predicted during a genome-wide screen for genes under regulation of the transcriptional regulator protein LaeA, which controls genes and even gene clusters dedicated to secondary metabolism [10, 13]. Prior to our biochemical investigations, we first verified involvement of *tdiA* and *tdiD* in this pathway and inactivated these genes by replacing them with the *pyroA* selection marker.

Inactivation of *tdiD* was accomplished by transformation of *A. nidulans* TN02A7 with the linear 4.5 kb *Eco*RI/*Hin*dIII insert of inactivation plasmid pKR2 to replace *tdiD* with a *pyroA* cassette. This manipulation eliminated the entire *tdiD* gene and 20 bp upstream of ATG and resulted in strain TMW3.7. Proper gene replacement was confirmed by Southern hybridization (not shown). *A. nidulans* produces two major, yet unrelated, metabolites, terrequinone A and sterigmatocystin, the latter being an aromatic polyketide and penultimate intermediate of the aflatoxin pathway. Upon comparison of the natural product spectrum of TMW3.7 versus the parental strain by HPLC and LC/MS, no variation in sterigmatocystin production was observed (Figure 3A). However, terrequinone A was only present in very moderate quantities in TMW3.7 yet unambiguously identifiable by LC/MS and by its UV-VIS spectrum. We therefore concluded that TdiD plays an important role for terrequinone A biosynthesis, although *A. nidulans* seems to harbor an enzyme that—albeit poorly—can complement the Δ*tdiD* genotype. We complemented *A. nidulans* TMW3.7 by transformation with plasmid pMW9 to introduce an intact *tdiD* copy back into the genome, to create strain TMW8.3. This complementation event restored terrequinone A biosynthesis close to wild-type level, as shown by HPLC (Figure 3A).

The *tdiA* inactivation was carried out in *A. nidulans* rNI773 by protoplast transformation with the linear 4.6 kb *Eco*RI/*Hin*dIII insert of inactivation plasmid pKR1, which deleted 43 bp upstream and 2351 bp within the *tdiA* reading frame and resulted in the Δ*tdiA* mutant TMW1.2, which was confirmed by Southern analysis as well (not shown). Inactivation of *tdiA* disabled terrequinone production quantitatively, and not even traces were detectable in HPLC chromatograms, while the sterigmatocystin production in the Δ*tdiA*-strain did not change (Figure 3A).

Enzyme Characterization

After *tdiA* and *tdiD* had experimentally been verified as part of the terrequinone biosynthetic cascade, we produced soluble TdiA- and TdiD-hexahistidine fusion proteins (Figure 4) in *E. coli* BL21(DE3) × pLysS transformed with plasmids pDH8 and pDH9, respectively. These expression plasmids harbor the corresponding cDNAs.

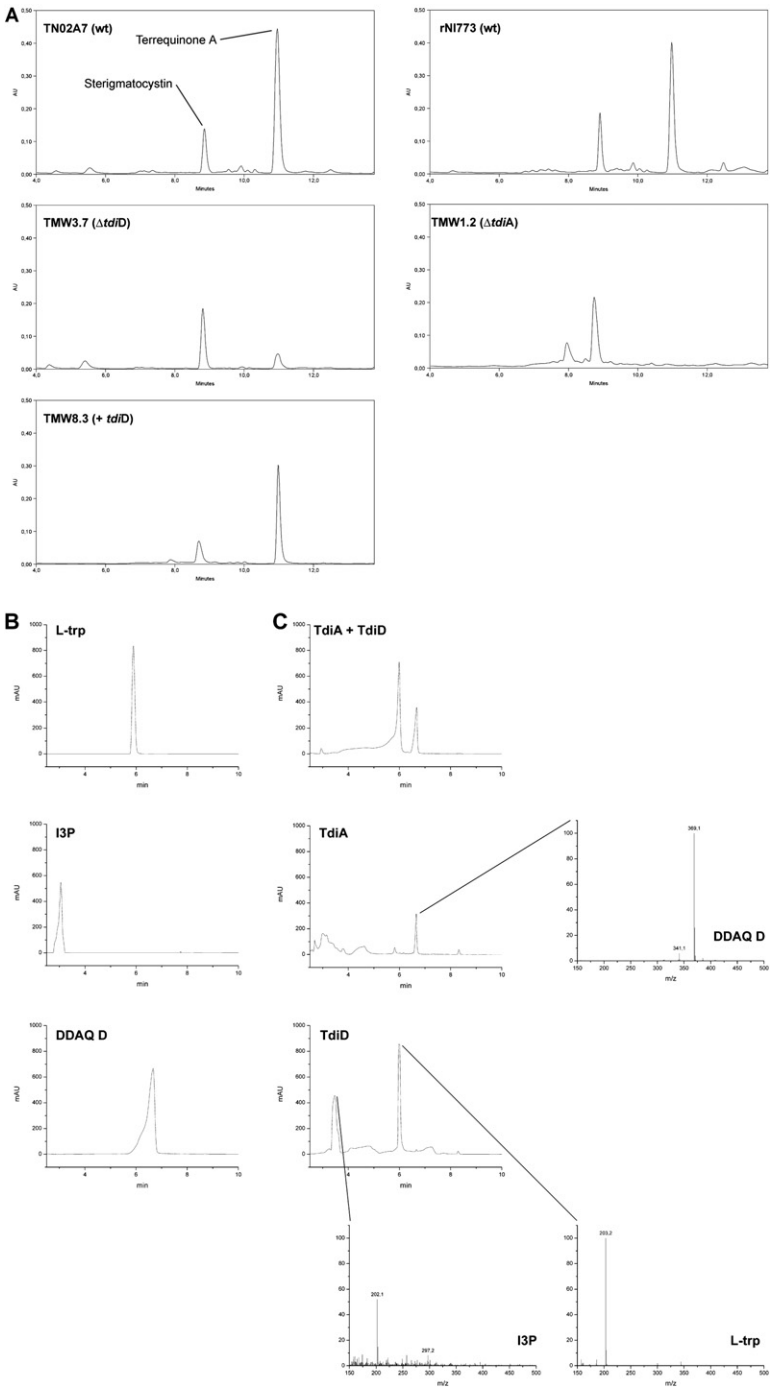

Figure 3. HPLC Chromatograms

(A) Natural product analyses of *A. nidulans* strains TN02A7 (WT), TMW3.7 (Δ*tdiD*), TMW8.3 (*tdiD* complementation), rNI773 (WT), and TMW1.2 (Δ*tdiA*), recorded at 280 nm. Sterigmatocystin elutes after 8.8 min, terrequinone A after 11.1 min, when applying the solvent gradient described in the Experimental Procedures.

(B) Authentic references: L-tryptophan (L-trp, retention time 5.9 min), indole-3-pyruvate (I3P, retention time 2.1 min), and di-demethyl-asterriquinone D (DDAQ D, retention time 6.6 min).

(C) Enzyme assays: coupled two-enzyme one-pot reaction (TdiA + TdiD), and single enzyme assays for TdiA and TdiD, respectively. APCI-MS traces (negative mode) are given for DDAQ D ($M\text{-}H^+$ = 369), L-tryptophan (L-Trp, $M\text{-}H^+$ = 203), and indole-3-pyruvate (I3P, $M\text{-}H^+$ = 202). Lines indicate the corresponding chromatographic peaks.

As the amino acceptor substrate for TdiD was unknown, we first tested a panel of α-keto acids, guided by characterized transaminases—mainly of nonfungal origin—involved in tryptophan degradation or natural product pathways, e.g., from *Agrobacterium tumefaciens* [14], the indolmycin producer *Streptomyces griseus* [15], *Corynebacterium glutamicum* [16] and *Neurospora crassa* [17], or from the mosquito *Anopheles gambiae* [18]. The tested amino acceptor substrates included pyruvic acid, 2-oxo glutaric acid, 2-oxo-butyric acid, 2-oxo-valeric acid, 4-hydroxy-phenylpyruvic acid, and phenylpyruvic acid. Significant transaminase activity with L-tryptophan as amino group donor was only detected in the presence of phenylpyruvic acid as amino acceptor, while all other compounds failed as adequate substrates and resulted in <5% indole-3-pyruvic acid formation, except 4-hydroxy-phenylpyruvic acid, which resulted in 15% conversion, compared to phenylpyruvic acid. Therefore, we report TdiD as the L-tryptophan:phenylpyruvate aminotransferase (EC 2.6.1.28), which catalyzes the first enzymatic

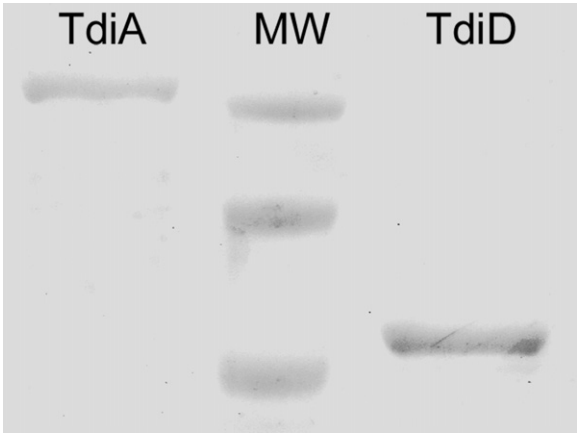

Figure 4. Electrophoretic Analysis of Heterologously Expressed Proteins

Hexahistidine-tagged enzymes TdiA (left lane, calculated mass: 107.6 kDa) and TdiD (right lane, calculated mass: 47.7 kDa) after SDS-polyacrylamide gel electrophoresis (12% Laemmli gel). Molecular weight markers on the center lane are (top to bottom) 97, 66, and 45 kDa, respectively.

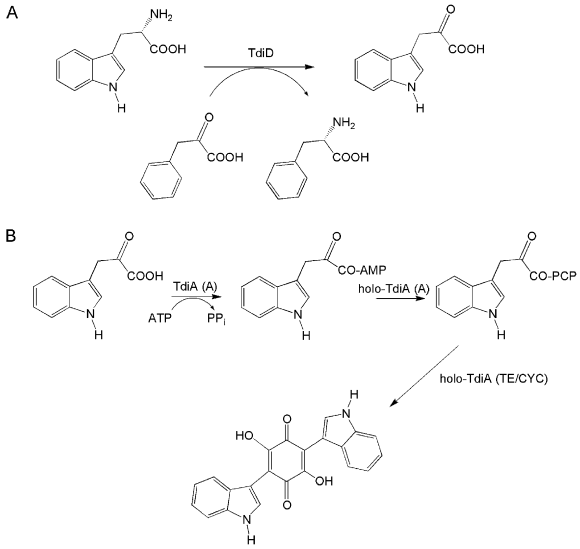

Figure 5. Reaction Schemes

The metabolic steps catalyzed by (A) the transaminase TdiD and (B) by the bis-indolylquinone synthetase TdiA constitute the initial events during bisindolylquinone biosynthesis.

step specific to the metabolic pathway toward terrequinone A (Figure 5A). To our knowledge, TdiD is the first fungal natural product transaminase to be characterized biochemically. The optimal temperature and pH value for TdiD was determined in vitro by product formation and assessed by HPLC. We found optimal product formation at 48°C, which appears somewhat out of the physiological range for an ubiquitous filamentous fungus, although even higher in vitro temperature optima have been reported for other transaminases [14, 18]. Further reactions were thus maintained at 48°C. Catalytic activity of TdiD was determined in 100 mM phosphate buffer at pH values ranging from 5.7 to 8.0. Optimal activity was observed at neutral pH, and no differences were found when the buffer was substituted for Tris-HCl. Kinetics characteristics are K_m = 3.02 ± 0.61 mM and k_{cat} = 1157 (± 104)/min for L-tryptophan; for phenylpyruvic acid, K_m = 1.43 (± 0.44) mM and k_{cat} = 548 (± 67)/min was found.

Although a big array of microbial adenylating enzymes has been investigated—the majority as integral domains of bacterial multimodular NRPSs for natural product or siderophore biosynthesis—the biochemistry of a bis-indolylquinone synthetase has not been described yet. Our strategy to investigate TdiA followed a two-step approach. First, we relied on the ATP-PP_i exchange assay to verify activity of heterologously expressed apo-TdiA and to record pH and temperature optimum. Optimal adenylation of indole-3-pyruvic acid took place at 42°C and at pH 6.5, although a plateau of >80% relative activity was identified for the range pH 6.0 to 7.0.

In a second step, we produced holo-TdiA through enzymatic phosphopantetheinyl (Ppant) transfer, catalyzed by the Ppant transferase Svp taken from the gram-positive soil bacterium *Streptomyces verticillus*, the producer of the antitumor drug bleomycin [19]. Holo-TdiA was employed to demonstrate product formation, i.e., DDAQ D, (Figure 5B) which was identified in HPLC analyses by its UV-spectrum, by mass spectrometry, and by comparison with an authentic sample (Figures 3B and 3C). Kinetics of TdiA were determined under optimal conditions reported above by measuring DDAQ D formation, and we found that holo-TdiA followed a typical Michaelis-Menten kinetic for indolepyruvic acid and saturating concentrations of ATP. The K_m value for indole-3-pyruvic acid was K_m = 1.16 ± 0.22 mM. The k_{cat} value was determined as k_{cat} = 69.9 ± 5.33/min. These results prove that TdiA possesses activity to cyclize monomeric indole-3-pyruvate into a quinoid structure. Moreover, we prove compatibility of the bacterial Svp with the fungal peptidyl carrier protein.

One-Pot Synthesis of Di-Demethylasterriquinone D

After optimal conditions were established for either enzyme, we explored the possibility of a combined two-step reaction to synthesize DDAQ D from two inexpensive substrates, L-tryptophan and phenylpyruvic acid. For indole-3-pyruvic acid, costs per mol are about 10-fold above those for phenylpyruvic acid and L-tryptophan (and pyridoxal 5-phosphate as cofactor) combined. This is why we sought to feed enzymatically generated indole-3-pyruvic acid into the process and why we did not simply rely on TdiA to synthesize DDAQ from indole-3-pyruvic acid.

Optimal synthesis of DDAQ D, mediated by the enzymes TdiD and TdiA, took place at 42°C in Tris-HCl buffer at pH 6.5. We used a 2-fold excess of phenylpyruvic acid as amino acceptor substrate of TdiD. In our pilot study, we found a 21% yield (a theoretical 100% yield would be the quantitative conversion of 2 mM L-tryptophan into 1 mM DDAQ D), as estimated by HPLC and

LC/MS, which provided evidence for DDAQ D production. Like above, authentic DDAQ D served as standard (Figures 3B and 3C).

DISCUSSION

In this publication, we report on the identification of *Aspergillus nidulans* TdiA as bis-indolyl-benzoquinone synthetase and of TdiD as an L-tryptophan:phenylpyruvic acid transaminase (Figure 5) along with their use for chemoenzymatic synthesis of didemethylasterriquinone D, the key precursor for the whole class of bis-indolylquinones, which is a class of cytotoxic, antidiabetes, and antiviral natural products.

Our in vitro studies clearly presented TdiD as the L-tryptophan:phenylpyruvate transaminase, whose biochemical properties and kinetic values are in good accordance with data available from the literature [14, 18]. This holds for the elevated temperature optimum of 48°C as well. As assessed by HPLC analyses, inactivation of the *tdiD* gene did not completely disrupt terrequinone A biosynthesis. As transamination is a crucial process during primary metabolism as well, e.g., during amino acid biosynthesis or breakdown, a presence of a second sufficiently flexible transaminase may account for the presence of basal cellular levels of indole-3-pyruvic acid, which supply TdiA with substrate. Upon searching the *A. nidulans* genome for further putative transaminase genes similar to *tdiD*, two clear hits (AN6338.2 and AN5041.3) were returned, both of which do not seem to be located in the obvious vicinity of genes dedicated to secondary metabolite production. Also, the *otaA* gene (AN1810.2) for the ornithine/acetylornithine aminotransferase ArgD involved in arginine biosynthesis in *A. nidulans* has been characterized yet not investigated for any tryptophan desaminase activity [20].

Promoted by fungal genomics, the past few years have seen identification of a wealth of fungal NRPS genes, e.g., 24 in *Aspergillus flavus* and 14 in *A. fumigatus* [21], or 11 in *Cochliobolus heterostrophus* (including the NRPS-polyketide synthase hybrid NPS7) [22]. This is in sharp contrast to the few fungal NRPSs that have been investigated biochemically, among those LPS2, which adenylates D-lysergic acid during ergotamine assembly [23], SimA of the cyclosporin pathway [24], GliP responsible for the gliotoxin skeleton [25], and the enniatin synthetase Esyn1 [26]. However, no data has been available at all for the class of C-domainless bis-indolylquinone synthetases. Also, TdiA-catalyzed dimerization of indole-3-pyruvic acid into a quinoid structure demonstrates carbon-carbon bond formation, which, in turn, implicates a novel chemistry for NRPSs: we assume a mechanism that follows a Claisen-type condensation with a nucleophilic attack on the thioester of the PCP-bound indole-3-pyruvate monomer by the enolate of a TE-bound indole-3-pyruvate, to establish the intermolecular C-C-bond between the two monomers. An intramolecular Dieckmann-condensation completes quinone formation and releases DDAQ D from the enzyme.

The "nonribosomal code," i.e., the specificity-conferring amino acid residues within the A-domain, remains to be determined. Yet, one would expect TdiA to follow a signature typical to aryl acid activating A-domains, such as DhbE (2,3-dihydroxybenzoate adenylation for bacillibactin biosynthesis in *Bacillus subtilis*) [27], or YbtE, a *Yersinia pestis* salicyl-AMP ligase [28]. Protein crystallography revealed the invariant aspartic acid residue in the core motif A4 (YxFDxS) of amino acid-AMP ligases serves to stabilize the α-amino group [29]. Further, this particular position was identified as instrumental to distinguish amino acid from arylic acid-AMP ligases, which possess a neutral asparagine residue instead (N235 in PheA terminology). Our sequence alignment identified residues and positions that follow neither the canonical amino acid signature nor the arylic acid "fingerprint" as the position in question is occupied by a valine (V239 in TdiA). However, assuming two gaps preceding motif A4, D237 of TdiA would align with "N235" residues in DhbE and EntE and confusingly indicate an amino acid signature. The core motif A4 in TdiA would then be represented by ^{236}VHMDHV^{239}, and the C245 residue would be moved further away from the salicylate/dihydroxybenzoate discriminating position (C/S239) if aligned with aryl acid activating domains. The TdiA A-domain amino acid sequence is markedly longer than its DhbE and YbtE counterparts: counting from N235 in DhbE (N222 in YbtE) as part of core motif A4, the hydrophobic end of core motif A6 (ARGYL) is 128 amino acid residues away, while TdiA possesses 151 amino acids. Therefore, the TdiA main chain may account for a structural situation in this critical portion that substantially deviates from DhbE or YbtE, and the computer-based results may reflect a suboptimal alignment that does not accurately bring structurally corresponding residues of TdiA and DhbE or YbtE into register. Eventually, only crystallographic studies can resolve this disparity and may shed more light on the specifics of the fungal nonribosomal code and the relevance of the cystein residue at position 245.

Homologs of *tdiA* and/or *tdiD* exist in numerous fungi and bacteria, including *Aspergillus terreus*, which harbors five *tdiA* homologs (XP_001210786, XP_001211182, XP_001217485, XP_001211993, and XP_001212741), *Aspergillus nidulans* itself (AN3396.3, a *tdiA* paralog), *Chaetomium globosum*, an allergenic ascomycete, which possesses *tdiA* and *tdiD* homologs clustered at the same chromosomal locus (XP_001230202 and XP_001230203), and a second *tdiA* homolog outside this locus (XP_001228818). *Phaeosphaeria nodorum*, an ascomycete that causes blotch disease in cereals, carries *tdiA* and *tdiD* homologs (EAT88825 and EAT88019, respectively). *Ralstonia solanacearum* is a devastating bacterial pathogen causing the bacterial wilt on solanaceous crops, such as potato, tomato, tobacco, and on other agriculturally important plants. This pathogen is of quarantine importance and object of rigorous pest response plans. *R. solanacearum* harbors a *tdiA* homolog (NP_522978), separated by four reading frames from the putative

transaminase gene NP_522983 in a predicted secondary metabolite gene cluster. Finally, *Burkholderia pseudomallei*, a bacterial pathogen in humans and causative agent of melioidosis, possesses a *tdiA* homolog (YP_336801). Alignments of the adenylation-domain motif A4 region of selected homologs are shown in Table 1. Although no literature is available, an enzymatic tandem of TdiA and TdiD orthologs can be envisioned as basis for the biosynthetic route toward terphenylquinone pigments in wood-rotting or mycorrhiza-forming basidiomycetes, as earlier feeding experiments with radiolabeled substances proved tyrosin and phenyllactic acid as precursors [30–32]. Taken together, TdiA and TdiD may serve as model enzymes for broadly distributed biosynthetic principles of secondary metabolism in commercially and agriculturally relevant microbes, beyond the class of bis-indolylquinones.

Multimodular enzymes, such as polyketide synthases or NRPSs rely on posttranslational phosphopantetheinylation (also referred to as priming) to convert the apoprotein, i.e., acyl-, aryl-, or peptidyl carrier domains into the functional holo-forms [33]. This priming is accomplished by dedicated Ppant transferases, which use coenzyme A as donor substrate. In this paper, we also demonstrate that the prokaryotic Ppant transferase Svp from *Streptomyces verticillus* ATCC15003, whose cellular function is priming the bleomycin NRPS, is promiscuous enough to convert the fungal apo-bis-indolylquinone synthetase TdiA into its holo-form. To our knowledge, this is the first demonstration of priming a eukaryotic NRPS-like enzyme with a prokaryotic PPtase. Also, our in vitro chemoenzymatic synthesis of di-demethylasterriquinone D represents the minimal variant of a hybrid *Streptomyces-Aspergillus* pathway and may stimulate research to expand the repertoire of combinatorial biosynthesis beyond the realm of actinomycete metabolites.

Enzymes from streptomycetes and other prokaryotic sources have successfully been used in pharmaceutical chemistry, as exemplified by in vitro glycorandomizing novel anticancer and antibiotic compounds, such as calicheamicin and vancomycin [34, 35], or in vivo approaches, as demonstrated for novobiocin [36]. Although the metabolic and structural wealth of fungal secondary metabolism is undoubted, we notice a paucity of efforts to tap into their rich reservoir of natural product enzymes for pharmaceutical purposes. This is even more surprising as a range of other fungal enzymes have found prominent places in biotechnology, e.g., laccases [37], dehydrogenases and lipases [38], or pyranose-2-oxidases [39]. Previous efforts to obtain bis-indolylquinones included either microbial fermentation [3, 4] or total synthesis. In either case, multistep purification procedures cannot be bypassed to remove byproducts or media ingredients. Protocols to synthesize bis-indolylquinones have been published [7, 8, 40, 41]. However, these routes lead to specific compounds—as does microbial fermentation of fungal producer strains—and do not serve as a platform technology from which to diverge toward as many different compounds as possible. In contrast, our protocol replicates the naturally occurring cascade and provides the pivotal intermediate toward a maximum diversity in terms of chemical structure and pharmacological activity via a facile two-step chemoenzymatic synthesis. Present efforts in our lab revolve around process scale-up and adding the diversifying prenyltransferase step, e.g., using the enzyme TdiB as a first proof of principle. Its gene is encoded in the *A. nidulans* terrequinone locus, it likely functions as a prenyltransferase, and is similar to a number of fungal prenyltransferases acting on indole-like structures. Many of them have already been characterized, and their genes have been cloned (reviewed in [42]). Sequence and biochemical information accumulating from these studies combined with increasingly sophisticated genomic mining techniques allow for identifying more prenyltransferase genes from a variety of species. Therefore, our technology presented here represents a viable route toward a multitude of candidate compounds in drug development.

SIGNIFICANCE

Due to diverse bioactivities, such as antiretroviral, antidiabetes, or cytostatic, fungal bis-indolylquinones represent an attractive class of fungal natural products. The first genetic locus for this class of secondary metabolites, the *tdi*-locus for terrequinone A biosynthesis in the filamentous fungus *Aspergillus nidulans*, has recently emerged through combined analytic, genomic, and transcriptomic efforts. In this publication, we report on the genetic and biochemical characterization of two enzymes: TdiD catalyzes the committing step during terrequinone A assembly, which is the transfer of an amino group from L-tryptophan onto phenylpyruvate. We also identified TdiA as bisindolyl-benzoquinone synthetase. The TdiA-catalyzed reaction implies new chemistry for NRPS-like enzymes due to C-C bond formation. By priming (i.e., transfer of a phosphopantetheinyl moiety) TdiA with the *Streptomyces* phosphopantetheinyl transferase Svp, we have demonstrated the feasibility of hybrid pathways with enzymes taken from the most important prokaryotic and most important eukaryotic source organisms of natural products. Also, as *tdiA* and *tdiD* homologs are found in the genomes of numerous other prokaryots and fungi, our results may provide a key to cryptic biosynthetic capabilities in a variety of microorganisms, among those clinically relevant human or crop plant pathogens. In this biochemical study of a bis-indolylquinone synthetase and a fungal natural product transaminase, we also present a one-pot two-enzyme chemoenzymatic route to di-demethylasterriquinone D—the universal intermediate for all bis-indolylquinones. This result provides a platform that is ready to be developed toward numerous members of this class of compounds with different bioactivities by simply adding specific tailoring enzymes, above all prenyltransferases, to the process.

EXPERIMENTAL PROCEDURES

General

Chemicals were purchased from Fluka, Sigma-Aldrich, and Roth. ^{32}P-labeled sodium phosphate (80.47 Ci/mmol) was obtained from PerkinElmer. Standard molecular biology procedures were performed as described [43]. Isolation of plasmid DNA from *E. coli*, and DNA restriction/ligation followed the protocols of the manufacturers of kits, enzymes, and reagents (Amersham-Pharmacia, Macherey-Nagel, Promega). Fungal strains are listed in Table S1 (see the Supplemental Data available with this article online). *Aspergillus* strains were routinely grown at 37°C on glucose minimal medium (GMM) [44] amended with appropriate supplements to maintain auxotrophs [45].

Genetic Manipulation of *Aspergillus nidulans*

The *tdiA* and the *tdiD* genes were inactivated separately and by disrupting the reading frame with linear constructs coding for the *A. nidulans pyroA* gene, flanked by 1 kb sequences representing DNA up- and downstream of *tdiA* and *tdiD*, respectively. PyroA complements the vitamine B_6-auxotrophic phenotype of *A. nidulans* strains rNI773 and TN02A7.

For *tdiA* inactivation, primer pairs tdiBF2/tdiBR2 for the 5′ flanking region and tdiBF1/tdiBR1 for the 3′ flank (which includes about 0.5 kb of the 3′ portion of the *tdiA* reading frame) were designed for PCR from chromosomal *A. nidulans* DNA. For *tdiD* flanking regions, primer pairs tdiEF1/tdiER1 and tdiEF2/tdiER2 were used. All primer sequences are listed in Table S2. *Pfu*-DNA polymerase was used for PCR amplification. 5′ flanks were cloned between the *Eco*RI/*Bam*HI sites (for the *tdiD* construct), and between *Eco*RI/*Kpn*I (for *tdiA*), the 3′ flanking regions were ligated to the *Pst*I/*Hin*dIII sites of plasmid p14 [46]. The DNA of flanking regions was checked by DNA sequencing.

The resulting plasmids were pKR1 for *tdiA*, and pKR2 for *tdiD* disruption. Linear gene disruption cassettes were obtained by releasing them from plasmids pKR1 or pKR2, by *Eco*RI/*Hin*dIII corestriction, followed by purification on an agarose gel. This DNA was used to transform *A. nidulans*. For *tdiA* inactivation, strain rNI773 [10] was used; *tdiD* was inactivated in TN02A7 [47]. Protoplast transformation of either strain followed standard protocols [10]. For each gene inactivation, about 50 transformants were prescreened by PCR for the gene replacement event. Chromosomal DNA from transformants was used to amplify the manipulated region by using the primer pairs tdiBF1/tdiBR2 for *tdiA* and tdiEF1/tdiER2 for *tdiD*. Putative positives were confirmed by Southern hybridization and HPLC-based natural product analysis. Strains TMW1.2 (Δ*tdiA*) and TMW3.7 (Δ*tdiD*) were used for further study.

To revert terrequinone A production to wild-type level in *A. nidulans* TMW3.7, this strain was complemented by transformation with plasmid pMW9, which carries a functional *tdiD* allele and complements uracil/uridine auxotrophy with the *Neurospora crassa pyr-4* gene as selection marker. To construct pMW9, a 3.5 kb PCR fragment (coding for *tdiD* and up- and downstream sequences) was amplified from chromosomal *A. nidulans* DNA by using the primer pair tdiEF1/tdiER2 and *Pfu*-DNA-polymerase. This fragment was restricted *Eco*RI/*Eco*RV and ligated to pBluescript (Stratagene) cut *Eco*RI/*Sma*I to create pMW8. DNA sequencing confirmed error-free amplification during PCR. The insert was removed from pMW8 by *Eco*RI/*Xba*I corestriction, and ligated to plasmid pMR18 (M. Reis and R. Fischer, personal communication), restricted equally, to yield pMW9. *A. nidulans* transformants were selected by culturing on GMM, supplemented with riboflavin (2.5 mg/l).

cDNA Cloning

The SV total RNA isolation system (Promega) was used to purify total RNA from *A. nidulans* TN02A7, grown under terrequinone-inducing conditions. First-strand cDNA synthesis was accomplished by using 25 pmol DNA-primer tdiB-CF1, 2.5 mM $MgCl_2$, 0.5 mM each dNTP, and ImProm reverse transcriptase (Promega). This was followed by a standard PCR reaction: 2.5 mM $MgCl_2$, 0.2 mM each dNTP, 40 pmol (each) primers tdiB-CF1 and tdiB-CR2, first-strand reaction as template, and 4U *Pfu* DNA-polymerase (Promega) in the buffer supplied with the enzyme, in a total volume of 100 μl with the following thermocycling parameters: initial denaturation, 2 min, 94°C; amplification, 35 cycles (94°C for 40 s, 62°C for 30 s, 72°C for 9 min); terminal hold, 8 min at 72°C. PCR products were electrophoretically separated on an agarose gel, and the desired bands excised, recovered with the Nucleospin Extract Kit (Macherey-Nagel), and ligated to the *Nde*I/*Eco*RI sites of pET28b (Novagen), to create pDH9. The insert was sequenced. Cloning of *tdiD*-cDNA followed essentially the same strategy but with primer *tdiE*-CF for first-strand synthesis and primer pair *tdiE*-CF/*tdiE*-CR for PCR for which the elongation time was set to 4 min. Cloning *tdiD*-cDNA to pET28b created pDH8.

Enzyme Overexpression and Purification

E. coli BL21(DE3) × pLysS (Stratagene) was transformed with pDH8 to produce His_6-tagged protein TdiD. One milliliter of an overnight culture in LB-medium, amended with chloramphenicol (30 mg/l) and carbenicillin (50 mg/l), was used to inoculate 100 ml of the same medium. The culture was incubated at 37°C on an orbital shaker at 180 rpm. The expression was induced by addition of 0.4 mM IPTG at an OD_{600} of 0.7, for 4 hr at 28°C, before collecting the biomass by centrifugation (4°C, 1,200 × g, 15 min). The cells were resuspended in lysis buffer (Na_2HPO_4/NaH_2PO_4 50mM, NaCl 300mM, imidazole 10 mM [pH 8.0]) and disrupted by passing the material twice through a French pressure cell (Thermo Scientific) at 16,000 psi working pressure. Cellular debris was removed by centrifugation at 4°C, 14,000 × g, for 15 min. The protein was purified by Ni-NTA (QIAGEN) affinity chromatography carried out following the QIAexpressionist manual. The pure enzyme was desalted on a PD-10 column (GE Healthcare) equilibrated with 100 mM Tris-Buffer (pH 7.5). The purification process was verified by SDS-Page analysis (12% Laemmli gels). The protein concentration was determined by the method of Bradford [48]. The identical procedure was applied for TdiA purification, except that induced bacterial cultures were maintained at room temperature. Purified enzymes were used for biochemical characterizations as described below.

Biochemical Characterization of TdiA

All reactions were run in triplicate. Adenylation domain: the TdiA adenylation domain was investigated by using the ATP-PP_i-exchange assay: it was carried out in a total volume of 100 μl at 42°C (varied from 4°C to 70°C to determine the temperature optimum) containing 100 mM Tris-HCl or phosphate buffers (pH 6.5) (varied from pH 5.7 to 8.0 used to determine the pH optimum), 6.25 mM $MgCl_2$, 125 μM EDTA, 6.25 mM ATP, 100 nM purified TdiA, 0.1 μM [^{32}P]-pyrophosphate, and 1 mM indole-3-pyruvic acid. After incubating for 20 min, the reaction was stopped and further processed as described [49].

Phosphopantetheinylation of TdiA: Apo-TdiA was converted to the holo-enzyme in vivo by using the *Streptomyces verticillus* Ppant transferase Svp encoded on plasmid pBS18 [19]. *E.coli* BL21(DE3) × pLysS was transformed with pDH8 and pBS18. The enzyme was expressed and purified as described for TdiA, followed by an additional size-exclusion filtration step with a Sartorius Vivaspin centrifugation device (cut-off limit 50 kDa) to remove Svp from the enzyme preparation.

Formation of didemethylasterriquinone D was accomplished in a 500 μl reaction set up as follows: 100 mM Tris-HCl (pH 6.5), 6.25 mM $MgCl_2$, 125 μM EDTA, 6.25 mM ATP, 100 nM purified holo-TdiA, and 1 mM indole-3-pyruvic acid, at 42°C, for 20 min (or various time points to record enzyme kinetics). Product formation was observed by HPLC analysis with gradient 1 (see below) and LC/MS.

Biochemical Characterization of TdiD

The enzyme assay was performed in a reaction mixture containing 1 mM L-tryptophan, 2 mM phenylpyruvate (or 2-oxobutyric acid, 2-ketoglutatate, oxaloacetate, p-hydroxyphenylpyruvate, or pyruvate), 0.5 μM pyridoxal phosphate, 100 mM Tris-HCl or phosphate buffers (pH 7.0) (or pH 5.7 to 8.0 to determine the pH optimum), and 10 nM purified enzyme. The incubation was carried out at 48°C (4°C

to 70°C during temperature profiling) and stopped after 30 min (or at different time points for recording enzyme kinetics) by snap freezing the sample in liquid nitrogen. The conversion to indole-3-pyruvate was monitiored by HPLC analysis with gradient 2 (see below) and LC/MS.

One-Pot Coupled Reaction TdiD-TdiA

The coupled reaction was performed in a mixture containing 100 mM Tris-HCl buffer (pH 6.5), 5 mM L-tryptophan, 10 mM phenylpyruvate, 10 mM ATP, 10 mM $MgCl_2$, 0.25 μM EDTA, and 0.5 mM pyridoxal phosphate. After incubating the mixture for 5 min at 42°C with 10 nM purified TdiD, purified holo-TdiA (10 nM) was added and incubated for another 25 min. The two-step conversion of L-tryptophan to didemethylasterrequinone D was verified by HPLC (gradient 1) and LC/MS. Authentic substance (kindly provided by Drs. Frank Petersen and Philipp Krastel, Natural Products Unit, Novartis Pharma AG, Basel, Switzerland) served as reference.

HPLC Analyses of Enzyme Assays

HPLC runs to analyze enzyme assays described above were perfomed on a Waters liquid chromatograph equipped with an Xbridge MS C-18 column (100 × 4.6 mm) and a C-18 guard column at 35°C: detection at 280 nm (diode array acquisition: 220–500 nm). Solvent A was water, solvent B acetonitrile. Two standard gradients (both at a flow rate of 0.8 ml/min) were applied. Gradient 1 was: within 2 min from 5% B to 35% B, within 10 min to 55% B, and then to 95% B within 2 min. Gradient 2 was: within 10 min from 5% to 10% B, followed by a ramp up to 95% B within 2 min. Analytical liquid chromatography-mass spectroscopy (LC/MS) was done on an Agilent 1100 integrated system equipped with a Zorbax Eclipse XDB C-8 column (150 × 4.6 mm, 5 μm particle size) and C-8 guard column essentially running the gradients described above. Mass spectrometry was performed with atmospheric pressure chemical ionization (APCI) in positive and negative mode and applying a capillary voltage of U = 3kV.

Aspergillus Natural Product Analysis

A. nidulans TMW1.2, TMW3.7, TMW8.3, as well as rNI773 or TN02A7 for reference were grown in 100 ml glucose minimal medium, dispensed into 300 ml Erlenmeyer flasks, and supplemented appropriately. The cultures were fermented at 37°C and 200 rpm, for 3 days. To determine differences in terrequinone A production between TMW8.3 and TN02A7, strains were cultivated and analyzed in triplicate. Upon harvest, the fermentation broth was centrifuged (10 min, 2,700 × g). The biomass was discarded. The supernatant was extracted with an equal volume of chloroform, and the organic layer evaporated in vacuo and then redissolved in 300 μl methanol and subjected to high performance liquid chromatography (HPLC). Analytical HPLC was performed on the equipment and solvents described above applying the following gradient: initial hold for 1 min at 45% B, within 3 min to 65% B, and then to 95% B within 10 min, at a flow rate of 0.5 ml/min.

Supplemental Data

Supplemental Data include genotypes of *Aspergillus* strains used during this study and oligonucleotide primer sequences and are available at http://www.chembiol.com/cgi/content/full/14/6/635/DC1/.

ACKNOWLEDGMENTS

We thank Professors Ben Shen (University of Wisconsin, Madison, WI), Reinhard Fischer (Technical University Karlsruhe, Germany), and Berl Oakley (Ohio State University, Columbus, OH) for kindly providing plasmids pBS18, pMR18, and *Aspergillus nidulans* TN02A7, respectively. We also thank Drs. Frank Petersen and Philipp Krastel (Novartis Pharma AG, Basel, Switzerland) for authentic didemethylasterriquinone D. This work was supported by the Deutsche Forschungsgemeinschaft DFG grant Ho 2515/3-1 and by the Fonds der Chemischen Industrie FCI. The authors declare that they have no conflicting financial interests.

Received: January 4, 2007
Revised: April 3, 2007
Accepted: May 8, 2007
Published: June 22, 2007

REFERENCES

1. Pelaez, F. (2004). Biological activities of fungal metabolites. In Handbook of Industrial Mycology, Z. An, ed. (New York, NY: Marcel Dekker), pp. 49–92.
2. Kaji, A., Iwata, T., Kiriyama, N., Nomura, M., and Miyamoto, K. (1998). Studies on the cytotoxicity of asterriquinone derivatives. J. Antibiot. *51*, 235–238.
3. Fredenhagen, A., Petersen, F., Tintelot-Blomley, M., Rösel, J., Mett, H., and Hug, P. (1997). Semicochliodinol A and B: inhibitors of HIV-1 protease and EGF-R protein tyrosine kinase related to asterriquinones produced by the fungus *Chrysosporium merdarium*. J. Antibiot. (Tokyo) *50*, 395–401.
4. Singh, S.B., Ondeyka, J.G., Tsipouras, N., Ruby, C., Sardana, V., Schulman, M., Sanchez, M., Pelaez, F., Stahlhut, M.W., Munshi, S., et al. (2004). Hinnuliquinone, a C2-symmetric dimeric nonpeptide fungal metabolite inhibitor of HIV-1 protease. Biochem. Biophys. Res. Commun. *324*, 108–113.
5. Zhang, B., Salituro, G., Szalkowski, D., Li, Z., Zhang, Y., Royo, I., Vilella, D., Diez, M.T., Pelaez, F., Ruby, C., et al. (1999). Discovery of a small molecule insulin mimetic with antidiabetic activity in mice. Science *284*, 974–977.
6. Velliquette, R.A., Friedman, J.E., Shao, J., Zhang, B.B., and Ernsberger, P.J. (2005). Therapeutic actions of an insulin receptor activator and a novel peroxisome proliferator-activated receptor gamma agonist in the spontaneously hypertensive obese rat model of metabolic syndrome X. J. Pharmacol. Exp. Ther. *314*, 422–430.
7. Liu, K., Wood, H.B., and Jones, A.B. (1999). Total synthesis of asterriquinone B1. Tetrahedron Lett. *40*, 5119–5122.
8. Pirrung, M.C., Li, Z., Park, K., and Zhu, J. (2002). Total syntheses of demethylasterriquinone B1, an orally active insulin mimetic, and demethylasterriquinone A1. J. Org. Chem. *67*, 7919–7926.
9. Arai, K., and Yamamoto, Y. (1990). Metabolic products of *Aspergillus terreus.* X. Biosynthesis of asterriquinones. Chem. Pharm. Bull. (Tokyo) *38*, 2929–2932.
10. Bok, J.W., Hoffmeister, D., Maggio-Hall, L.A., Murillo, R., Glasner, J.D., and Keller, N.P. (2006). Genomic mining for *Aspergillus* natural products. Chem. Biol. *13*, 31–37.
11. *Aspergillus* Sequencing Project (2006). *Aspergillus nidulans* Database (http://www.broad.mit.edu/annotation/genome/aspergillus_nidulans/Home.html).
12. Schwarzer, D., Finking, R., and Marahiel, M.A. (2003). Nonribosomal peptides: from genes to products. Nat. Prod. Rep. *20*, 275–287.
13. Bok, J.W., and Keller, N.P. (2004). LaeA, a regulator of secondary metabolism in *Aspergillus* spp. Eukaryot. Cell *3*, 527–535.
14. Sukanya, N.K., and Vaidyanathan, C.S. (1964). Aminotransferases of *Agrobacterium tumefaciens*. Transamination between tryptophan and phenylpyruvate. Biochem. J. *92*, 594–598.
15. Speedie, M.K., Hornemann, U., and Floss, H.G. (1975). Isolation and characterization of tryptophan transaminase and indolepyruvate C-methyltransferase. Enzymes involved in indolmycin biosynthesis in *Streptomyces griseus*. J. Biol. Chem. *250*, 7819–7825.
16. Marienhagen, J., Kennerknecht, N., Sahm, H., and Eggeling, L. (2005). Functional analysis of all aminotransferase proteins inferred from the genome sequence of *Corynebacterium glutamicum*. J. Bacteriol. *187*, 7639–7646.
17. Jakoby, W.B., and Bonner, D.M. (1956). Kynurenine transaminase from *Neurospora*. J. Biol. Chem. *221*, 689–695.

18. Rossi, F., Lombardo, F., Paglino, A., Cassani, C., Miglio, G., Arca, B., and Rizzi, M. (2005). Identification and biochemical characterization of the *Anopheles gambiae* 3-hydroxykynurenine transaminase. FEBS J. *272*, 5653–5662.

19. Sanchez, C., Du, L., Edwards, D.J., Toney, M.D., and Shen, B. (2001). Cloning and characterization of a phosphopantetheinyl transferase from *Streptomyces verticillus* ATCC15003, the producer of the hybrid peptide-polyketide antitumor drug bleomycin. Chem. Biol. *8*, 725–738.

20. Dzikowska, A., Swianiewicz, M., Talarczyk, A., Wisniewska, M., Goras, M., Scazzocchio, C., and Weglenski, P. (1999). Cloning, characterisation and regulation of the ornithine transaminase (*otaA*) gene of *Aspergillus nidulans*. Curr. Genet. *35*, 118–126.

21. Payne, G.A., Nierman, W.C., Wortman, J.R., Pritchard, B.L., Brown, D., Dean, R.A., Bhatnagar, D., Cleveland, T.E., Machida, M., and Yu, J. (2006). Whole genome comparison of *Aspergillus flavus* and *A. oryzae*. Med. Mycol. Suppl. *44*, 9–11.

22. Lee, B.N., Kroken, S., Chou, D.Y., Robbertse, B., Yoder, O.C., and Turgeon, B.G. (2005). Functional analysis of all nonribosomal peptide synthetases in *Cochliobolus heterostrophus* reveals a factor, NPS6, involved in virulence and resistance to oxidative stress. Eukaryot. Cell *4*, 545–555.

23. Correia, T., Grammel, N., Ortel, I., Keller, U., and Tudzynski, P. (2003). Molecular cloning and analysis of the ergopeptine assembly system in the ergot fungus *Claviceps purpurea*. Chem. Biol. *10*, 1281–1292.

24. Lawen, A., and Zocher, R. (1990). Cyclosporin synthetase. The most complex peptide synthesizing multienzyme polypeptide so far described. J. Biol. Chem. *265*, 11355–11360.

25. Balibar, C.J., and Walsh, C.T. (2006). GliP, a multimodular nonribosomal peptide synthetase in *Aspergillus fumigatus*, makes the diketopiperazine scaffold of gliotoxin. Biochemistry *45*, 15029–15038.

26. Haese, A., Pieper, R., von Ostrowski, T., and Zocher, R. (1994). Bacterial expression of catalytically active fragments of the multifunctional enzyme enniatin synthetase. J. Mol. Biol. *243*, 116–122.

27. May, J.J., Kessler, N., Marahiel, M.A., and Stubbs, M.T. (2002). Crystal structure of DhbE, an archetype for aryl acid activating domains of modular nonribosomal peptide synthetases. Proc. Natl. Acad. Sci. USA *99*, 12120–12125.

28. Gehring, A.M., DeMoll, E., Fetherston, J.D., Mori, I., Mayhew, G.F., Blattner, F.R., Walsh, C.T., and Perry, R.D. (1998). Iron acquisition in plague: modular logic in enzymatic biogenesis of yersiniabactin by *Yersinia pestis*. Chem. Biol. *5*, 573–586.

29. Conti, E., Stachelhaus, T., Marahiel, M.A., and Brick, P. (1997). Structural basis for the activation of phenylalanine in the non-ribosomal biosynthesis of gramicidin S. EMBO J. *16*, 4174–4183.

30. Read, G., Vining, L.C., and Haskins, R.H. (1962). Biogenetic studies on volucrisporin. Can. J. Chem. *40*, 2357–2361.

31. Mosbach, K., Guilford, H., and Lindberg, M. (1974). The terphenyl quinone polyporic acid: production, isolation, and characterization. Tetrahedron Lett. *17*, 1645–1648.

32. Liu, J.K. (2006). Natural terphenyls: developments since 1877. Chem. Rev. *106*, 2209–2223.

33. Marahiel, M.A., Stachelhaus, T., and Mootz, H.D. (1997). Modular peptide synthetases involved in nonribosomal peptide synthesis. Chem. Rev. *97*, 2651–2674.

34. Zhang, C., Griffith, B.R., Fu, Q., Albermann, C., Fu, X., Lee, I.K., Li, L., and Thorson, J.S. (2006). Exploiting the reversibility of natural product glycosyltransferase-catalyzed reactions. Science *313*, 1291–1294.

35. Griffith, B.R., Langenhan, J.M., and Thorson, J.S. (2005). "Sweetening" natural products via glycorandomization. Curr. Opin. Biotechnol. *16*, 622–630.

36. Galm, U., Dessoy, M.A., Schmidt, J., Wessjohann, L., and Heide, L. (2004). In vitro and in vivo production of new aminocoumarins by a combined biochemical, genetic, and synthetic approach. Chem. Biol. *11*, 173–183.

37. Baldrian, P. (2006). Fungal laccases—occurrence and properties. FEMS Microbiol. Rev. *30*, 215–242.

38. Müller, M. (2005). Chemoenzymatic synthesis of building blocks for statin side chains. Angew. Chem. Int. Ed. Engl. *44*, 362–365.

39. Giffhorn, F. (2000). Fungal pyranose oxidases: occurrence, properties and biotechnical applications in carbohydrate chemistry. Appl. Microbiol. Biotechnol. *54*, 727–740.

40. Shimizu, S., Yamamoto, Y., and Koshimura, S. (1982). Antitumor activity of asterriquinones from *Aspergillus* fungi. IV. An attempt to modify the structure of asterriquinones to increase the activity. Chem. Pharm. Bull. (Tokyo) *30*, 1896–1899.

41. Pirrung, M.C., Liu, Y., Deng, L., Halstead, D.K., Li, Z., May, J.F., Wedel, M., Austin, D.A., and Webster, N.J.G. (2005). Methyl scanning: total synthesis of demethylasterriquinone B1 and derivatives for identification of sites of interaction with and isolation of its receptor(s). J. Am. Chem. Soc. *127*, 4609–4624.

42. Hoffmeister, D., and Keller, N.P. (2007). Natural products of filamentous fungi: enzymes, genes, and their regulation. Nat. Prod. Rep. *24*, 393–416.

43. Sambrook, J., and Russell, D.W. (2000). Molecular Cloning: A Laboratory Manual, Third Edition (Cold Spring Harbor, NY: Cold Spring Harbor Laboratory Press).

44. Shimizu, K., and Keller, N.P. (2001). Genetic involvement of a cAMP-dependent protein kinase in a G protein signaling pathway regulating morphological and chemical transitions in *Aspergillus nidulans*. Genetics *157*, 591–600.

45. Adams, T.H., and Timberlake, W.E. (1990). Developmental repression of growth and gene expression in *Aspergillus*. Proc. Natl. Acad. Sci. USA *87*, 5405–5409.

46. Osmani, A.H., May, G.S., and Osmani, S.A. (1999). The extremely conserved *pyroA* gene of *Aspergillus nidulans* is required for pyridoxine synthesis and is required indirectly for resistance to photosensitizers. J. Biol. Chem. *274*, 23565–23569.

47. Nayak, T., Szewczyk, E., Oakley, C.E., Osmani, A., Ukil, L., Murray, S.L., Hynes, M.J., Osmani, S.A., and Oakley, B.R. (2006). A versatile and efficient gene-targeting system for *Aspergillus nidulans*. Genetics *152*, 1557–1566.

48. Bradford, M. (1976). A rapid and sensitive method for the quantitation of microgram quantities of protein utilizing the principle of protein-dye binding. Anal. Biochem. *72*, 248–254.

49. Van Lanen, S.G., Dorrestein, P.C., Christenson, S.D., Liu, W., Ju, J., Kelleher, N.L., and Shen, B. (2005). Biosynthesis of the beta-amino acid moiety of the enediyne antitumor antibiotic C-1027 featuring beta-amino acyl-S-carrier protein intermediates. J. Am. Chem. Soc. *127*, 11594–11595.

